

# Transparent film thickness measurement by three-wavelength interference method: An extended application of Global Model Fitting algorithm

Katsuichi Kitagawa  
Toray Engineering Co. Ltd.  
1-1-45, Oe  
Otsu, 520-2141, Japan

**Abstract-** Conventional transparent film thickness measurement methods such as spectroscopy are basically capable of measuring a single point at a time, and the spatial resolution is limited. We propose a novel areal film thickness measurement method by extending the Global Model Fitting algorithm developed for three-wavelength interferometric surface profiling. It estimates the film thickness distribution from a color image captured by a color camera with three-wavelength illumination. The validity of the proposed method is demonstrated by computer simulations and actual experiments.

## I. INTRODUCTION

Conventional transparent film thickness measurement methods such as spectroscopy and ellipsometry are basically capable of measuring a single point at a time, and the spatial resolution is limited. To overcome this problem, researchers developed various kinds of areal measurement techniques which can measure the film thickness using a TV camera. A typical example is imaging spectrophotometry [1,2]. Another example is an ellipsometric imaging system [3,4]. These methods require an expensive camera or a complex mechanism.

Another approach is to use the interference color. The interference color phenomenon of thin film is seen in soap bubbles, and the relation between the color and thickness are long investigated, as seen in the Newton color chart. This relation has been used for measuring semiconductor film thickness [5,6], flying height of magnetic head [7] and lubricant film thickness [8,9]. A typical example is the lubricant film thickness measurement system described by Eguchi et al. [9], in which a color camera captures the interference image and the film thickness at each pixel is estimated from its hue by using the calibration data obtained in advance.

However, these techniques have been seldom used in industry. The most serious problem is that they require a frequent calibration because the color-thickness relation depends on the various environmental conditions such as the illumination and the target film structure. Another problem is their narrow unambiguous measurement range of a few hundred nm caused by a cyclic repetition of colors depending on the thickness.

To overcome these problems, we propose a novel areal film thickness measurement method, named GMFT (Global Model Fitting for Thickness), by extending the Global Model Fitting algorithm developed for three-wavelength interferometric surface profiling [10,11]. We proved the validity of the proposed method by computer simulations and actual experiments.

## II. PRINCIPLE OF THE GMFT METHOD

Our algorithm consists of two steps; a flowchart is shown in Fig. 1. Step 1 is the GMFT method, which estimates the thickness of each pixel from its color information. Because of the high computational cost, this method is applied to a limited number of pixels in practical use. Step 2 is another method, named ACOS, which calculates the thickness of the other pixels in a shorter time, by using the information obtained from Step 1. The information can also be applicable to other images captured under the same optical conditions. For that reason it can be called a recipe.

### A. The GMFT method

#### (a) Relationship between color and thickness

Consider light incident on a thin film and reflected by both

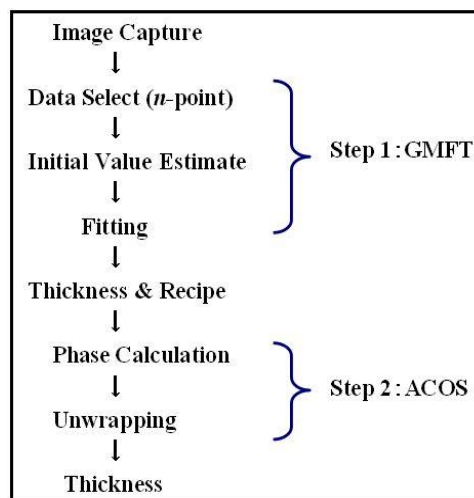


Figure 1. Flowchart of the proposed method.

the upper and lower boundaries. Ignoring multiple reflections, we can obtain the intensity of the sum of the two reflected waves as

$$I(\lambda) = I_1(\lambda) + I_2(\lambda) + 2\sqrt{I_1(\lambda)I_2(\lambda)} \cos\{\delta(\lambda)\}, \quad (1)$$

where  $I_1$  and  $I_2$  are the intensities of the waves,  $\lambda$  is the wavelength, and  $\delta$  is the phase difference between them. Assuming a uniform refractive index,  $n(\lambda)$ , and normal incidence of light, the optical path difference (OPD) between the two reflections from a thin film is  $OPD = 2n(\lambda)t$ , where  $t$  is the thickness of the layer. Therefore the phase difference for light reflected from the two surfaces is  $\delta(\lambda) = 2\pi OPD/\lambda = 4\pi n(\lambda)t/\lambda$ . For a nondispersive medium (i.e.,  $n(\lambda) = n$ ) we obtain

$$I(\lambda) = I_1(\lambda) + I_2(\lambda) + 2\sqrt{I_1(\lambda)I_2(\lambda)} \cos(4\pi nt/\lambda). \quad (2)$$

Let's consider a case of three-wavelength (B, G, R) illumination. Assuming that  $I_1 = I_2 = 1/2$ , and  $\lambda_B = 470$  nm,  $\lambda_G = 560$  nm,  $\lambda_R = 600$  nm, we calculated the theoretical intensities of each wavelength for the optical thickness range 0-1000 nm, and then obtained the synthesized color chart. The results are shown in Fig. 2. Please note that the color change is due to the cyclic variation of BGR signals according to the film thickness. This means that we can estimate the film thickness from the BGR signals, instead of the color information itself.

Three-wavelength BGR signals can be obtained by an interference color imaging system shown in Fig. 3. This is almost the same configuration as that of three-wavelength single-shot interferometry reported by Kitagawa [12]. The details of the actual apparatus is shown later in section IV.

#### (b) The GMFT algorithm

Although a case of three wavelengths was considered in Fig. 2, in the following equations we assume a more generalized expression of  $m$  wavelengths.

When we capture interference images of  $m$  wavelengths, the observed intensity  $g(i, j)$  at point  $i$  ( $i = 1, 2, \dots, n$ ) and wavelength  $j$  ( $j = 1, 2, \dots, m$ ) is given by the following model:

$$g(i, j) = a(j)[1 + b(j)\cos\{\phi(i, j)\}], \quad (3)$$

where  $a(j)$  and  $b(j)$  are the DC bias and the modulation of the waveform, respectively, and  $\phi(i, j)$  is the phase given by

$$\phi(i, j) = 4\pi nt(i)/\lambda_j, \quad (4)$$

where  $n$  is the known refractive index,  $t(i)$  is the thickness, and  $\lambda_j$  is the wavelength of the wavelength number  $j$ . Putting (4)

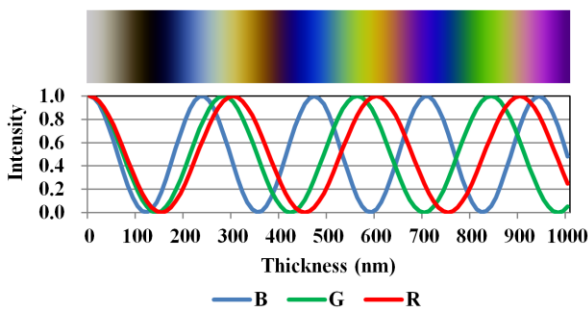


Figure 2. BGR intensities and synthesized color chart as a function of film thickness.

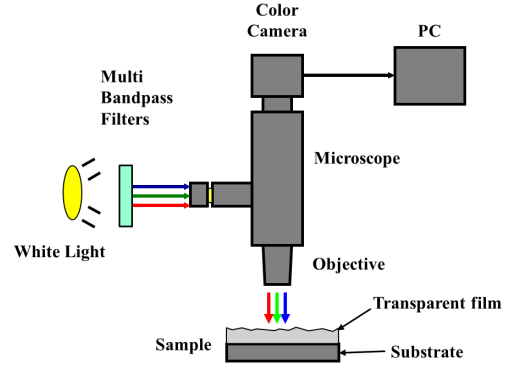


Figure 3. Optics of three-wavelength interference color imaging.

into (3) gives the following model:

$$g(i, j) = a(j)[1 + b(j)\cos\{4\pi nt(i)/\lambda(j)\}]. \quad (5)$$

This model is derived under the assumption that the waveform parameters  $a(j)$  and  $b(j)$  are constant in the field of view (FOV) and dependent only on the wavelength. This assumption will be almost always valid when the target surface is homogeneous.

The unknown parameters  $a(j)$ ,  $b(j)$  and  $t(i)$  can be estimated using the following least-square fitting equation:

$$J[a(j), b(j), t(i)] = \sum_{i=1}^n \sum_{j=1}^m [g(i, j) - g_{ij}]^2, \quad (6)$$

where  $g(i, j)$  is the model intensity defined by (5) and  $g_{ij}$  is the observed intensity.

This non-linear least-square problem can be solved by any numerical methods. In this paper, we used the Solver program in MS Excel for the computer simulation. For the actual experiments, we used our own program based on the Davidon-Fletcher-Powell algorithm [13].

#### (c) Necessary conditions

Let us consider the necessary conditions to obtain the unknown parameters  $a(j)$ ,  $b(j)$  and  $t(i)$ . When the number of wavelengths is  $m$  and the number of points is  $n$ , the total number of unknown parameters is  $2m+n$ . Since  $m$  values are observed at one point, the necessary condition for the solution is  $mn \geq 2m+n$ . Then, the number of points must be

$$n \geq 2m/(m-1). \quad (7)$$

This means  $n \geq 4$  in the case of  $m = 2$ , and  $n \geq 3$  in the case of  $m = 3$ . When  $n = 2m/(m-1)$ , then the problem becomes a  $(2m+n)$ -order non-linear simultaneous equation, and when  $n > 2m/(m-1)$ , then the problem becomes a  $(2m+n)$ -order non-linear least-square problem.

Fig. 4 illustrates the principle of this algorithm in the case of three wavelengths and  $n$ -points. From  $3n$  observed intensities,  $(n+6)$  unknown parameters, i.e.,  $n$ -point thicknesses and six waveform parameters, are estimated.

Please note that to avoid the problem becoming ill-conditioned and obtain good estimation, it is advisable to select the points so that their thickness distribution becomes wide.

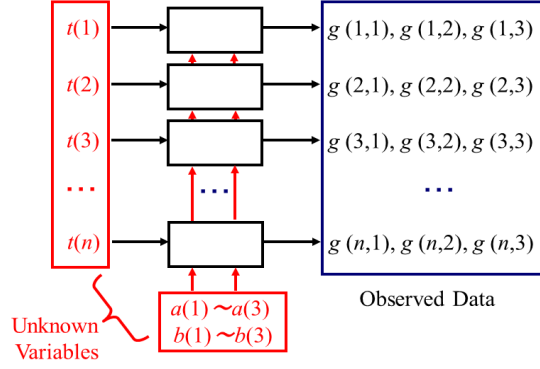


Figure 4. Principle of the GMFT method (in the case of three wavelengths and  $n$ -point fitting).

#### (d) Initial estimates

To find solutions to the non-linear least-square problem described in the previous section, we use an iterative technique, which requires initial estimates that will allow us to search for the minimum. Since the model function of (5) contains a cosine function, the error function has a lot of local minimum. Therefore, it is essential to make good initial estimates.

In this paper,  $a(j)$  is set to be the average of the observed values and the modulation,  $b(j)$ , is set to be the range of observed values divided by  $2a(j)$ . The thickness,  $t(i)$ , is a rough estimate which is given usually by a priori knowledge of the target sample.

#### B. The ACOS Algorithm

The computational cost of the non-linear least-square problem is very high, so the method becomes impractical when the number of points is large. Therefore, we use the GMFT algorithm as the first step with a small number of points, for example, under one hundred, and then the thicknesses of the other points are calculated as the second step by the following method, named the “arccosine(ACOS)” method, which uses the estimated waveform parameters from the first step.

#### (a) Phase estimation

When the waveform parameters are given, the phase is obtained from the observed intensity by the following equation derived from (3):

$$\phi(i, j) = \cos^{-1}[\{g_{ij} / a(j) - 1\} / b(j)], \quad (8)$$

where  $\cos^{-1}$  is the arccosine function and its value range is  $[0, \pi]$ . When the argument of the function is not within  $[-1, 1]$ , the function is undefined. In this case, the argument is approximated as  $-1$  or  $1$ .

#### (b) Phase unwrapping

From the phase data, the thickness,  $t(i, j)$ , is obtained by

$$t(i, j) = (1/n)[\pm\phi(i, j) / 2\pi + N(i, j)](\lambda_j / 2), \quad (9)$$

where  $N(i, j)$  is the fringe order (integer), which is estimated by the coincidence method. The principle of this method is the same as the so-called exact fractions method [14] for gauge block length measurement by multi-wavelength interferometry.

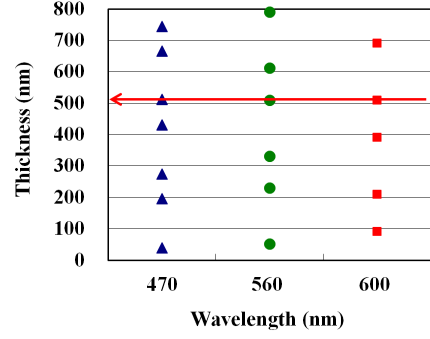


Figure 5. Phase unwrapping by the coincidence method.

Fig. 5 shows an experimental example of using this method. For each wavelength, the thicknesses with different orders are plotted. The unknown orders are determined so that the three candidate thicknesses match best. In this case, the thickness is estimated as 510 nm. It should be noted that the phase is obtained by the arccosine function, not by the arctangent function. Therefore, there are two candidate thicknesses for each fringe order, as shown in Fig. 5.

### III. COMPUTER SIMULATIONS

#### A. Test method

A three-wavelength interference color image was synthesized with the following conditions: (a) image size =  $50 \times 50$  pixels; (b) pixel size =  $1 \mu\text{m}$ ; (c) wavelength = 470, 560, 600 nm; (d) target surface = sphere with 1-mm radius, with a small square protrusion of thickness 50 nm and size  $4 \times 4$  pixels; (e) waveform parameters of  $a = 100$  and  $b = 1$ . The target surface is shown in Fig. 6, and the synthesized image is shown in Fig. 7.

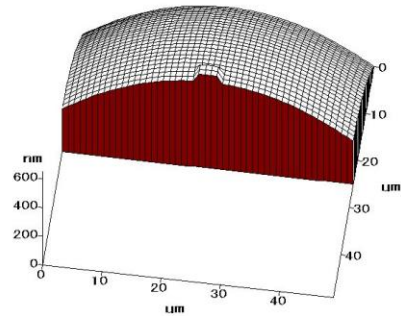


Figure 6. Target surface used for computer experiments. (cross-sectioned).

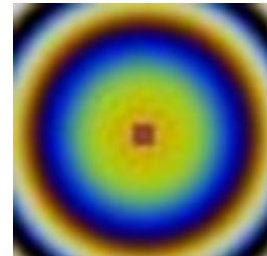


Figure 7. Synthesized color image.

All the computations were done in MS Excel with a Windows PC. The non-linear least-square fitting in the GMFT method was executed by the Solver program in MS Excel.

We performed two experiments. The first one used three points for fitting, and the second one used 50 points. The coordinates of the sampled points were (5, 25), (15, 25), (25, 25) in the first test and (1, 25), (2, 25), ..., (50, 25) in the second test.

### B. Test results

#### (a) Three-point fitting

The BGR images are shown in Fig. 8 with three points used for fitting. The intensity values are shown in Fig. 9. The initial estimates of the thicknesses are set at 95% of the true ones. The estimated thicknesses are shown in Fig. 10 with the initial and true values. The detailed results are shown in Table I. The parameters and thicknesses are estimated correctly.

#### (b) 50-point fitting

We estimated the thickness profile of 50 points along the  $y = 25$  using 50 points for the GMFT fitting. The intensities are shown in Fig. 11. The initial estimates are set to be the true thicknesses minus 50 nm. The thicknesses are estimated correctly, as shown in Fig. 12. Please note that the small protrusion of  $4 \times 4$  pixel size is measured correctly without any loss in spatial resolution.

#### (c) Thickness estimation by the ACOS method

Next, we estimated the thickness profile of 50 points along the  $y = 25$  using the recipe obtained by the GMFT 3-pt fitting. From the intensities shown in Fig. 11, the phases are obtained as shown in Fig. 13. Then the thicknesses are estimated correctly, as shown in Fig. 14.

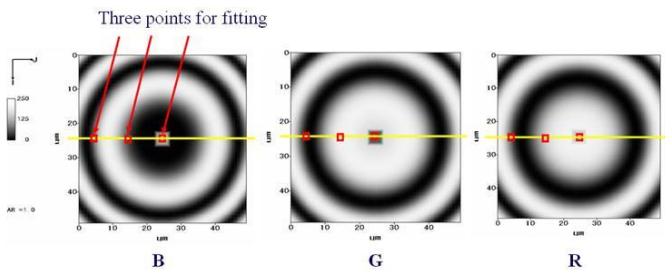


Figure 8. BGR images and three points used for fitting.

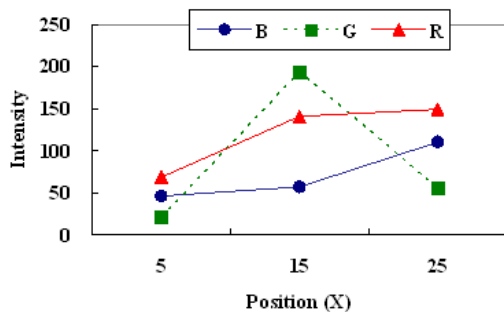


Figure 9. Observed intensities for the three-point fitting.

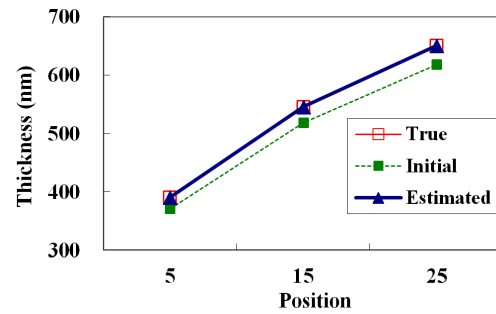


Figure 10. Estimated thicknesses by the three-point fitting.

TABLE I  
ESTIMATED VARIABLES BY THE THREE-POINT FITTING

VARIABLES		TRUE	INITIAL	ESTIMATED	ERROR(%)
$t$	$t(1)$	390	371	390	0.00
	$t(2)$	545	518	545	0.00
	$t(3)$	650	618	650	0.00
$a$	B	100	79	100	0.00
	G	100	108	100	0.00
	R	100	109	100	0.00
$b$	B	1.00	0.41	1.00	0.00
	G	1.00	0.80	1.00	0.00
	R	1.00	0.37	1.00	0.00

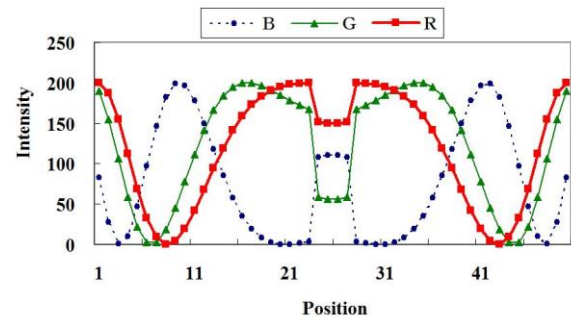


Figure 11. Intensity profiles of 50 points along  $y = 25$ .

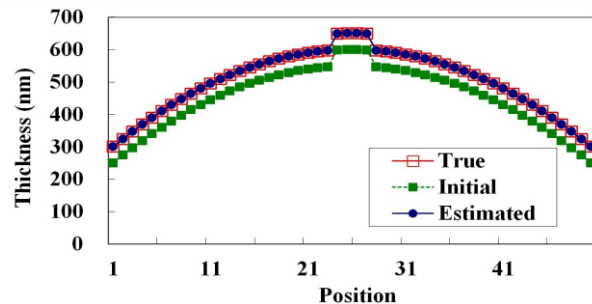


Figure 12. Estimated thicknesses of 50 points by the GMFT 50-pt fitting.

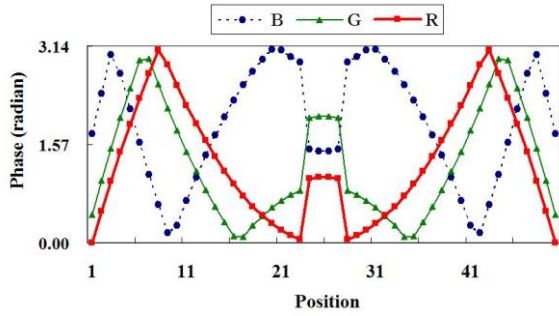


Figure 13. Phase profiles calculated by the ACOS method.

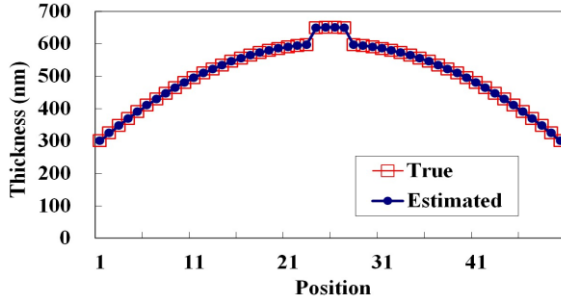


Figure 14. Estimated thicknesses of 50 points by the ACOS method with the recipe obtained by the GMFT 3-pt fitting.

#### IV. ACTUAL EXPERIMENTS

##### A. Test method

The experimental apparatus is shown in Fig. 15. The illumination unit consists of a halogen lamp and a multi-bandpass filter as shown in Fig. 2. The spectral transmittance of the filter is shown in Fig. 16. The central wavelengths were 470 nm, 560 nm and 600 nm, and their bandwidths were 10nm. The camera was a three-CCD color camera (Hitachi, HV-F22CL) with 1360×1024 pixels. Its spectral sensitivity is shown in Fig. 17 with the wavelengths of the illumination. The captured image was stored in a PC memory as an integer value from 0 to 255. The color crosstalk was compensated by the crosstalk compensation algorithm reported in [11]. We installed the GMFT algorithm in the Windows PC using C language.

In our experiments, a calibrated step wafer (Mikropack, Germany) was used, which consists of a 100 mm Si-wafer with 6 silicon dioxide ( $\text{SiO}_2$ ;  $n=1.46$ ) steps between 0 nm and 500 nm as shown in Fig. 18. The captured microscopic images of six step areas were stitched together to get an image shown in Fig 19.

The non-linear least-square equation in the GMFT algorithm was solved using the Davidon-Fletcher-Powell method [13]. The data for fitting were six points, each at the center of the step area, as shown in Fig 19. The initial thickness values were set to be the nominal values. The thickness range of each point was set to be the nominal value  $\pm 50$  nm.

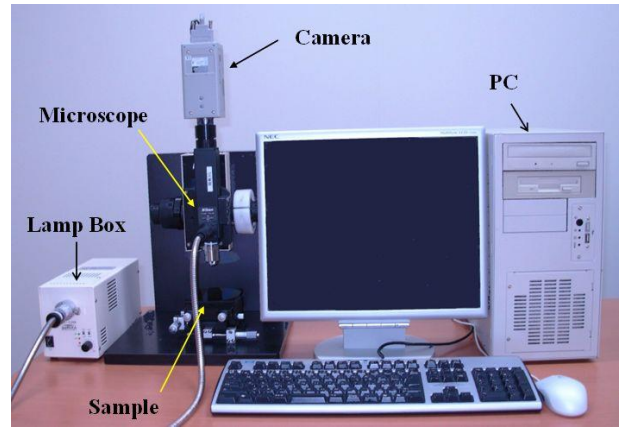


Figure 15. Experimental apparatus.

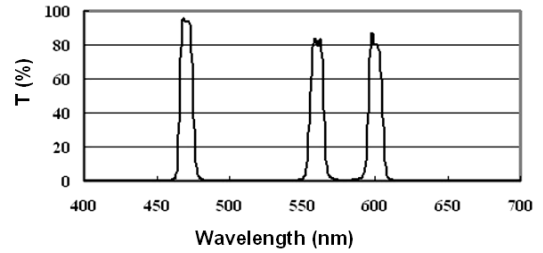


Figure 16. Spectral transmittance of the multi-bandpass filter.

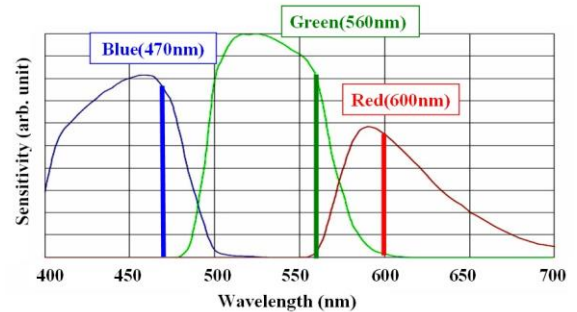


Figure 17. Camera sensitivity and three wavelengths.

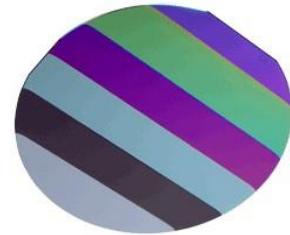


Figure 18. Target thickness standard.

In the second step, we calculated the thickness distribution of the whole area of 1344×1024 pixels by using the parameters obtained in the first step.

##### B. Test results

From the 6-point intensity data, their thicknesses were estimated by the GMFT method. The results are shown in Table II. Fig. 20 shows a good correlation between the nominal and measured thicknesses.

Then, the thickness distribution of the whole area was measured by the ACOS method. As shown in Fig. 21, good agreement between the measured and predicted thickness distributions was obtained.

The total calculation time for 1344×1024 pixels was about 1.2 s including 6 ms of the GMFT fitting using a C language program running on a Windows PC (3.4GHz Intel Core i7-2600 CPU). Because the calculation of the ACOS method is pixel-independent, the speed would be very much improved by a parallel processing technique.

## V. DISCUSSION

### A. Thickness measurement resolution

In our previous study [11], we made a theoretical analysis on the measurement resolution of the GMF method. The result suggests that we can expect approximately 1-nm optical thickness resolution in a case of 8-bit intensity scale, provided that the noise level of the observed intensity is within a few gray levels. With 10-bit intensity scale, sub-nm resolution would be achieved.

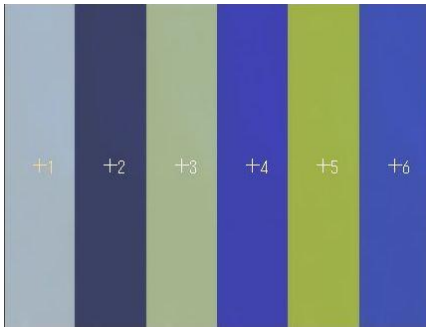


Figure 19. Stitched color image of thickness standard, and 6 points for GMFT fitting (shown in white numbers).

TABLE II  
RESULTS OF GMFT FITTING

Variables		Initial	Estimated
$t$	$t(1)$	0	0
	$t(2)$	100	107
	$t(3)$	200	197
	$t(4)$	300	300
	$t(5)$	400	396
	$t(6)$	500	504
$a$	B	144	133
	G	125	122
	R	113	113
$b$	B	0.43	0.47
	G	0.47	0.49
	R	0.47	0.46

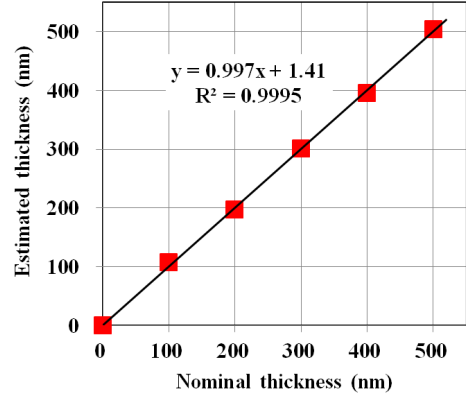


Figure 20. Estimated thicknesses by GMFT fitting.

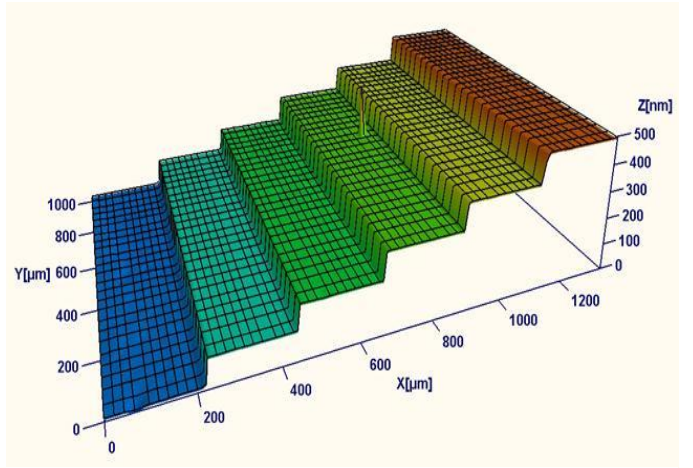


Figure 21. Measured thickness distribution of the thin film reference wafer with 0-500 nm thickness steps.

### B. Effect of the initial estimates

As mentioned in II A (d), the error function has a lot of local minima. Therefore, it is necessary to start with the best initial estimates possible for the parameters to avoid getting trapped in local minima. In our previous study [11], we investigated the problem of how accurately the parameters must be estimated to get the true solution. The conclusion suggests that the initial estimate of the optical thickness must be within  $\pm 100$  nm of the true value.

We can avoid this local minimum problem by a global optimization algorithm, such as the multi-start method in which a series of starting points are selected within the defined lower and upper bounds. Although this method takes more computing time, it is only in the GMFT calculation, and has no effect on the ACOS calculation.

### C. Maximum measurable thickness

In the GMFT method, theoretically there is no limit to the thickness range. We note that the estimated thickness is dependent on its initial estimate, as discussed above.

The issue of the maximum measurable thickness of the ACOS method is almost the same as that with three-

wavelength spatial carrier interferometry [12], because the thickness is determined by spectral unwrapping using the phases of three wavelengths. The unambiguous range depends on various factors, including wavelengths, electronic noises and optical errors. As for the wavelengths, the 470-560-600 nm combination used in this paper was selected by Kitagawa [12] as the optimum one giving an unambiguous range of approximately 4  $\mu\text{m}$ . Therefore, the measurement range of at least 4  $\mu\text{m}$  can be expected.

## VI. CONCLUSION

We have proposed a new interferometric thickness profiling technique, the Global Model Fitting for Thickness (GMFT) method, which enables us to measure a thickness distribution from a single color image captured by a CCD camera. It is based on a model-fitting algorithm and estimates the model parameters and the thicknesses of plural points simultaneously from their multi-wavelength intensity data.

When the number of the wavelengths is three, the minimum number of data points is three, and a total of nine unknown parameters including the thicknesses of three points are estimated by least-square fitting. Once the waveform parameters are estimated by this technique, they can be used for thickness estimation of the points other than the fitted points, which can be executed by a much simpler and faster algorithm using the arccosine function. The validity of the proposed method has been proved by computer simulations and actual experiments.

The most significant feature of this technique is that no preliminary calibration is required, that is, if there are at least three points of different thicknesses in the test sample, a kind of self-calibration is achieved. Other advantages include (1) high-speed areal measurement, (2) wide measurement range, and (3) low cost and simple optics. We are currently working on extending our technique for practical applications.

## REFERENCES

- [1] T. S. Hyvarinen, E. Herrala, and A. Dall'Ava, "Direct sight imaging spectrograph: a unique add-on component brings spectral imaging to industrial applications," *Proc. SPIE*, vol. 3302, pp. 165-175, 1998.
- [2] M. Ohlidal, V. Cudek, I. Ohlidal, and P. Klapetek, "Optical characterization of non-uniform thin films using imaging spectrophotometry," *Proc. SPIE*, vol. 5963, pp. 596329, October 2005.
- [3] G. Jin, R. Jansson, and H. Arwin, "Imaging ellipsometry revisited: developments for visualization of thin transparent layers on silicon substrates," *Rev. Sci. Instr.*, vol. 67, pp. 2930-2936, August 1996.
- [4] T. Sato et al., "Compact ellipsometer employing a static polarimeter module with arrayed polarizer and wave-plate elements," *Appl. Opt.*, vol. 46, pp. 4963-4967, July 2007.
- [5] S. Parthasarathy, D. Wolfe, E. Hu, S. Hackwood, and G. Beni, "A color vision system for film thickness determination," *Proc. IEEE Conf. Robotics and Automation*, vol. 4, pp. 515-519, March 1987.
- [6] D. Birnie, "Optical video interpretation of interference colors from thin transparent films on silicon," *Materials Letters*, vol. 58, pp. 2795-2800, September 2004.
- [7] M. Kubo, Y. Ohtsubo, N. Kawashima, and H. Marumo, "Head slider flying height measurement using a color image processing technique," *JSME international journal, Series 3*, vol. 32, pp. 264-268, June 1989.
- [8] M. Hartl, I. Krupka, R. Poliscuk, and M. Liska, "Computer-aided evaluation of chromatic interferograms," *Fifth International Conference in Central Europe on Computer Graphics and Visualization*, pp. 45-54, February 1997.
- [9] M. Eguchi and T. Yamamoto, "Film thickness measurement using white light spacer interferometry and its calibration by HSV color space," *Proceedings of the 5th International Conference on Tribology*, pp. 20-22, September 2006.
- [10] K. Kitagawa, "Multi-wavelength single-shot interferometry without carrier fringe introduction," *Proc. SPIE*, vol. 8000, pp. 800009, July 2011.
- [11] K. Kitagawa, "Single-shot surface profiling by multi-wavelength interferometry without carrier fringe introduction," *Journal of Electronic Imaging*, vol. 21, pp. 021107, May 2012.
- [12] K. Kitagawa, "Fast surface profiling by multi-wavelength single-shot interferometry," *International Journal of Optomechatronics*, vol. 4, pp. 136-156, June 2010.
- [13] R. Fletcher, and M. J. D. Powell, "A rapidly convergent descent method for minimization," *Computer Journal*, vol. 6, pp. 163-168, August 1963.
- [14] C. Tilford, "Analytical procedure for determining lengths from fractional fringes," *Appl. Opt.*, vol. 16, pp. 1857-1860, July 1977.

This is the final manuscript of  
Katsuichi Kitagawa: "Transparent film thickness measurement by three-wavelength interference method: An extended application of Global Model Fitting algorithm",  
Proc. of Int'l Workshop on Mechatronics (MECATRONICS-REM) 2012, pp. 94-100  
(Paris, Nov. 2012)

<http://ieeexplore.ieee.org/xpl/articleDetails.jsp?reload=true&arnumber=6450993>